

# Nitrogen-Rich Liquid Phase Regions in the Ln–Si–Al–O–N (Ln = Nd, Sm, Gd, Dy, Er and Yb) Systems

W. Y. Sun, H. Y. Tu, P. L. Wang & D. S. Yan

The State Key Lab on High Performance Ceramics and Superfine Microstructure, Shanghai Institute of Ceramics, Academia Sinica, Shanghai, People's Republic of China

(Received 27 March 1996; revised version received 30 June 1996; accepted 15 July 1996)

## Abstract

*Liquid phase regions at 1700°C with nitrogen concentration higher than 40 eq% in the systems Ln–Si–Al–O–N (Ln = Nd, Sm, Gd, Dy, Er and Yb) have been determined. All the systems possess extensive liquid phase regions at 40 eq% N. With increasing nitrogen content, the liquid phase regions contract towards Si-rich compositions. The maximum solubility of nitrogen in the Ln-sialon liquids is slightly above 50 eq%, which is much higher than in Y-sialon liquid, of which the highest nitrogen concentration was determined to be slightly above 30 eq%. With increasing Z-value of rare earth elements, the liquid phase regions contract towards the Si- and Ln-rich side. © 1997 Elsevier Science Limited. All rights reserved.*

## 1 Introduction

It is well known that metal oxides are necessary for the densification of silicon nitride ceramics. During sintering, the metal oxide additives and silicon nitride (which unavoidably contains a small amount of silica as impurity), form an eutectic melt which aids densification. The liquid composition affects the resulting microstructure and hence the properties of the final ceramics; it also determines the nature of grain-boundary crystalline phases after heat-treatment. The importance of using rare earth oxides for the densification of silicon nitride ceramics has been recognized during recent years. Not only are they very effective for densification, but also they can be accommodated in the  $\alpha$ -sialon lattice, thus providing an opportunity for decreasing the transient liquid phase content after sintering, and hence reducing the amount of residual grain boundary glass. Investigation of bulk glasses reported that viscosity, glass

transition temperature, refractive index, and resistance to devitrification all increase initially with increasing nitrogen concentration.<sup>1</sup> This is because  $N^{3-}$  substitutes for  $O^{2-}$  in the glass network, thereby increasing the amount of crosslinking.<sup>2</sup> Therefore, in ceramics materials, an intergranular glassy phase with increasing N becomes more refractory and improves the mechanical properties, especially at high temperatures. The alternative advantage of using rare earth oxides as sintering additives for  $Si_3N_4$ -based ceramics was thought to be the formation of N-rich Ln-sialon (Ln–Si–Al–O–N) glasses as grain boundary phase. Among the rare earth oxides,  $Sm_2O_3$  and  $Nd_2O_3$  are the two commonly used as sintering additives and modifiers for forming  $\alpha$ -sialon  $(Ln_xSi_{12-(m+n)}Al_{m+n}O_nN_{16-n})$ .<sup>3–6</sup> For these reasons, the phase relationships and the formation of crystalline phases in the Sm(Nd)–Si–Al–O–N systems have been studied in more detail.<sup>7–9</sup> Our previous work<sup>9</sup> on Sm-sialon glasses indicated that Sm-sialon glasses can accommodate more nitrogen than the Mg-sialon and Y-sialon glasses and the maximum solubility of nitrogen in the Sm-glasses is slightly above 40 eq%. As noted, the determination of the glass-forming region strongly depends on the experimental conditions. In our laboratory,<sup>9</sup> the specimens cooled down in a furnace with a cooling rate down to 1200°C within 5 min (from 1700°C). If the specimens could be quenched in N atmosphere, the glass-forming region is expected to be more extensive. Nevertheless, the extension of the liquid phase region depends on the temperature alone. The liquid compositions melted at high temperatures normally give glasses and crystalline phases after cooling down. The cooling speed only affect the crystallization of the crystalline phases. Therefore, at the same temperature, the liquid phase region is considered to be more extensive than the glass-forming

region. For design and fabrication of nitride ceramics, information about the liquid phase region seems more desirable. The present paper reports the N-rich liquid phase regions in the Ln-Si-Al-O-N (Ln = Nd, Sm, Gd, Dy, Er and Yb) systems at 1700°C. For comparison, the N-rich liquids in the Y-Si-Al-O-N system was also determined in the present work.

## 2 Experimental Procedure

The starting powders used were  $\alpha$ -Si<sub>3</sub>N<sub>4</sub> (Starck H1), AlN (containing 1.2% O), Al<sub>2</sub>O<sub>3</sub> (99.99%), SiO<sub>2</sub> (99.9%), Ln<sub>2</sub>O<sub>3</sub> (Ln = Nd, Sm, Gd, Dy, Er, Yb, 99.99%) and Y<sub>2</sub>O<sub>3</sub> (99.99%). The oxygen contents of the nitride powders were taken into account in computing the compositions. The compositions were ground under absolute alcohol using an agate mortar and pestle. The mixed powders were dried and pressed into pellets. Each specimen was embedded in BN in a small graphite crucible which was then packed in a powder mixture of Si<sub>3</sub>N<sub>4</sub> and BN in a large crucible to suppress weight loss. A graphite resistance furnace was used to melt the specimens in nitrogen atmosphere. After holding at 1700°C for 1.5 h, the crucibles were removed from the hot zone allowing a faster cooling rate down to 1200°C within 5 min. All the fired specimens were examined by X-ray diffraction technique. Some of the X-ray analysis data are summarized in Tables 1–8.

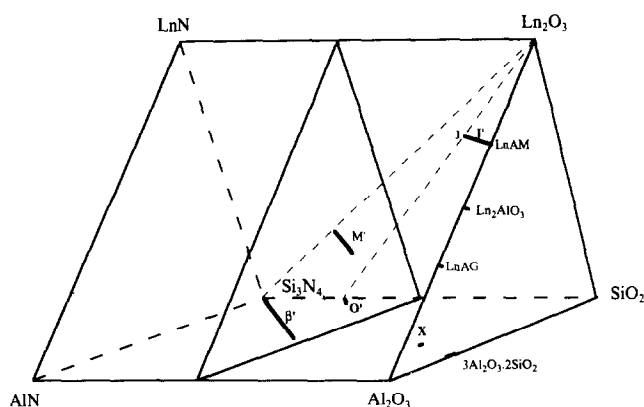


Fig. 1. Representation of vertical section with constant N : O in the Ln-Si-Al-O-N system.

## 3 Results and Discussion

Based on the work<sup>9</sup> on the Sm-sialon glasses which indicated the maximum solubility of nitrogen in the glasses as being slightly above 40 eq%, the highest nitrogen content in Sm-sialon liquid is expected to be higher than this value. Therefore, in the present work, three vertical sections with constant N content of 40, 50 and 55 eq% were explored (the vertical section with constant N in the Ln-Si-Al-O-N systems is represented in Fig. 1). The compositions, weight loss, crystalline phases and appearance after firing are summarized in Tables 1–3. Based on the appearance of specimens after firing (1700°C, 1.5 h), the compositions were judged as melted, half-melted and unmelted (they are represented by dots, ellipsoids and circles

Table 1. Compositions explored in the Sm-Si-Al-O-N system with 40 eq% N

No.	Compositions (eq%)			W.L. (wt%)	Crystalline phases*	Appearance
	Sm	Si	Al			
Sm-1	5	85	10	3.2	o's	half-melted, swollen
Sm-2	5	30	65	3.2	$\beta_{60}$ ms; Al <sub>2</sub> O <sub>3</sub> m; 15R w	unmelted
Sm-3	10	80	10	2.8	o'm	melted, swollen
Sm-4	10	60	30	3.4	$\beta$ 's	melted, swollen
Sm-5	10	50	40	2.7	$\beta$ 's	melted, swollen
Sm-6	10	40	50	2.3	$\beta_{60}$ s; Al <sub>2</sub> O <sub>3</sub> m	melted
Sm-7	10	30	60	0.3	15R mw; Al <sub>2</sub> O <sub>3</sub> mw	half-melted, swollen
Sm-8	20	75	5	3.4	o'vw; $\beta$ 'vw;	melted
Sm-9	20	70	10	1.0	M's; K m	melted, swollen
Sm-10	20	60	20	0.5	None	melted, swollen
Sm-11	20	55	25	3.5	None	melted
Sm-12	20	50	30	0.7	$\beta$ 's	melted, swollen
Sm-13	20	40	40	0.5	LnAlO <sub>3</sub> w	melted, swollen
Sm-14	30	60	10	2.1	M's; K s	melted
Sm-15	30	50	20	1.4	M's	melted
Sm-16	30	40	30	0.4	M's; LnAlO <sub>3</sub> m	melted, swollen
Sm-17	30	30	40	0	LnAlO <sub>3</sub> vs; M's	unmelted
Sm-18	35	42.5	22.5	0	M'vs; LnAlO <sub>3</sub> m; H w	melted
Sm-19	40	50	10	0.7	M'vs; H m	unmelted
Sm-20	40	30	30	3.3	M'vs; LnAlO <sub>3</sub> vs	unmelted

\* $\beta$ ' =  $\beta$ -Sialon; o' = o-Sialon; 15R = AlN-polypolyd (SiAl<sub>4</sub>O<sub>2</sub>N<sub>4</sub>); K = K-phase (Ln<sub>2</sub>Si<sub>2</sub>N<sub>2</sub>O<sub>4</sub>); M' = melitite solid solution (Ln<sub>2</sub>Si<sub>3-x</sub>Al<sub>x</sub>O<sub>3+x</sub>N<sub>4-x</sub>); H = H-phase (Ln<sub>10</sub>(SiO<sub>4</sub>)<sub>6</sub>N<sub>2</sub>).

**Table 2.** Compositions explored in the Sm-Si-Al-O-N system with 50 eq% N

No.	Compositions (eq%)			W.L. (wt%)	Crystalline phases*	Appearance
	Sm	Si	Al			
Sm-21	5	75	20	2.7	o'm; $\beta'$ w; X w; $\alpha$ w	unmelted, swollen
Sm-22	10	80	10	2.4	o'mw; $\beta'$ vw; $\alpha$ vw	melted
Sm-23	10	70	20	3.2	$\alpha$ w; $\beta'$ vw	melted
Sm-24	10	60	30	2.9	$\beta'$ mw	melted, swollen
Sm-25	10	50	40	1.9	$\beta'$ m; 15R w	melted, swollen
Sm-26	20	75	5	1.6	H m; $\beta$ vw	half-melted
Sm-27	20	70	10	1.6	H m; $\beta$ w	melted
Sm-28	20	60	20	2.5	M'mw; $\beta'$ w; U w	melted
Sm-29	20	50	30	1.0	M'ms; U m	melted
Sm-30	20	40	40	1.6	M'vs; U m	half melted
Sm-31	30	50	20	1.2	M'vs; U vw	half-melted
Sm-32	30	40	30	0.7	M's; LnAlO <sub>3</sub> m	unmelted

\* $\alpha$  =  $\alpha$ -Si<sub>3</sub>N<sub>4</sub>; X = X-phase (Si<sub>3</sub>Al<sub>6</sub>O<sub>12</sub>N<sub>2</sub>); U = U-phase (Ln<sub>3</sub>Si<sub>3</sub>Al<sub>3</sub>O<sub>12</sub>N<sub>2</sub>); for others see Table 1.

**Table 3.** Compositions explored in the Sm-Si-Al-O-N system with 55 eq% N

No.	Compositions (eq%)			W.L. (wt%)	Crystalline phases*	Appearance
	Sm	Si	Al			
Sm-33	10	80	10	1	o'w; $\beta'$ vw; $\alpha$ vw	melted, swollen
Sm-34	10	70	20	1	undetermined	unmelted
Sm-35	20	70	10	0	H m; $\beta'$ vw; $\alpha'$ tr.	half-melted
Sm-36	20	60	20	0	undetermined	unmelted

\*See Tables 1 and 2.

respectively in the figures). As indicated in Fig. 2, the liquid phase region at 40 eq% N is relatively extensive, but after cooling most of the compositions contained more or less crystalline phases. Only the compositions around Sm:Si:Al:O:N = 20:(60–55):(20–25):60:40 were composed of a full amorphous phase, which are actually located in the glass-forming region with the highest N concentration.<sup>9</sup> With increasing N content, the liquid phase region contracts towards silicon-rich compositions. On the 55 eq% N section, only one composition, Sm:Si:Al:O:N=10:80:10:45:55,

was observed to melt (Table 3). Therefore, the maximum solubility of N in the Sm-sialon liquid can be figured to be between 50 and 55 eq% N. Our previous work<sup>7</sup> on the subsolidus phase relationships in the Ln<sub>2</sub>O<sub>3</sub>-Si<sub>3</sub>N<sub>4</sub>-AlN-Al<sub>2</sub>O<sub>3</sub> (Ln = Nd, Sm) systems indicated that these two systems have the same phase relationships. Therefore, in the liquid phase formation, the Nd-Si-Al-O-N system is considered to be very similar to the Sm-Si-Al-O-N system. As expected, the liquid formation in the Nd-sialon system is very close to that in the Sm-system (see Fig. 4).

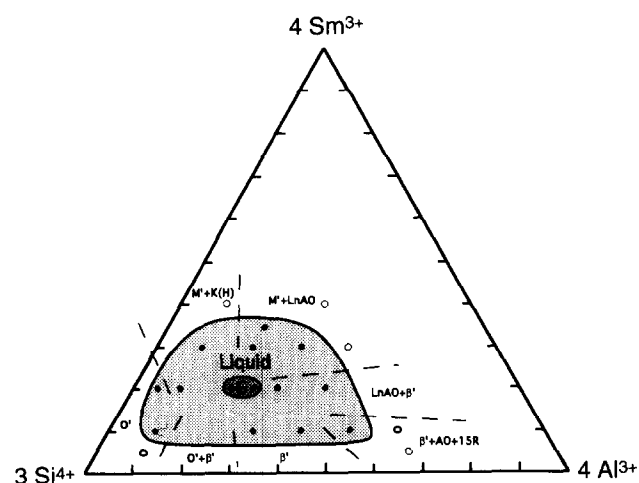


**Fig. 2.** Sm-sialon liquid phase region (1700°C) and neighbouring crystalline phases at 40 eq% N (G: glass; AO: Al<sub>2</sub>O<sub>3</sub>; LnAO: LnAlO<sub>3</sub>; see Table 1).

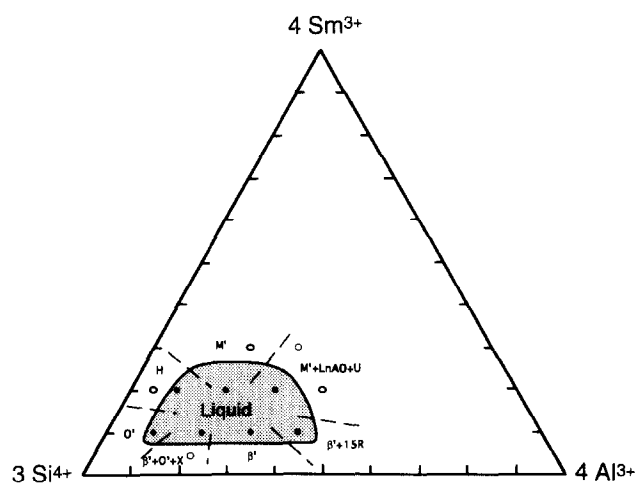


**Fig. 3.** Sm-sialon liquid phase region (1700°C) and neighbouring crystalline phases at 50 eq% N (see Table 2 and Fig. 2).

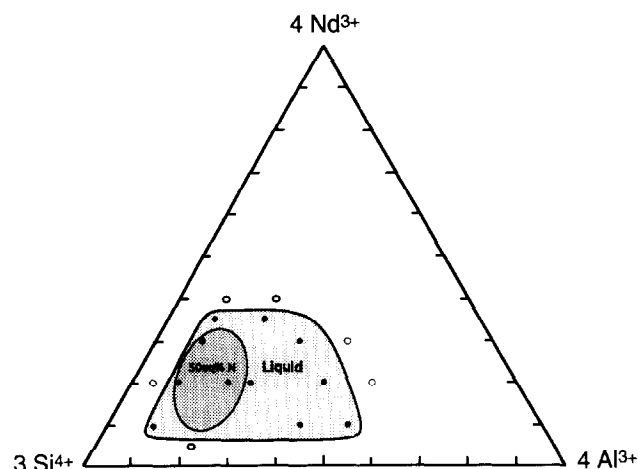


Fig. 4. Nd-sialon liquid phase regions (1700°C) at 40 eq% and 50 eq% N.

The liquid phase regions (at 40 and 50 eq% N) for the other Ln-Si-Al-O-N systems (Ln = Gd, Dy, Er, Yb) are represented in Figs 5–8. As indicated, at 40 eq% N, the liquid phase regions are all extensive. With increasing N content, the liquid phase regions gradually contract towards

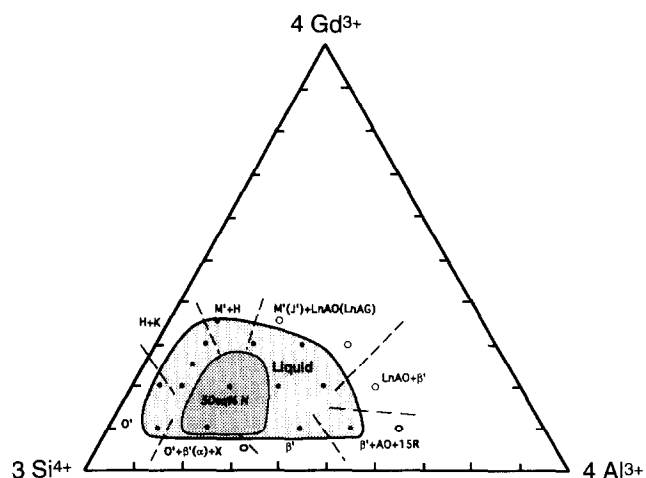


Fig. 5. Gd-sialon liquid phase regions (1700°C) at 40 eq% N (with neighbouring crystalline phases indicated, see Tables 4 and Fig. 2) and 50 eq% N.

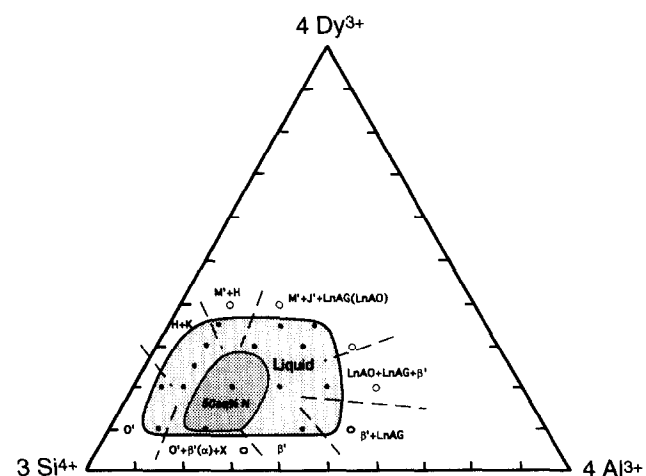


Fig. 6. Dy-sialon liquid phase regions (1700°C) at 40 eq% N (with neighbouring crystalline phases indicated, see Table 5 and Fig. 2) and 50 eq% N.

silicon-rich compositions. The maximum solubility of N in the Ln-Si-Al-O-N liquid can be figured to be slightly above 50 eq%. In comparison with each other, it can be seen that, as in compound formation and phase relationships,<sup>7,8,10</sup> the Ln-systems with neighbouring rare earth elements are also more similar. As indicated in Figs 5 and 6, the Gd-Si-Al-O-N and Dy-Si-Al-O-N systems have very similar liquid phase compositions and crystalline phases occurring around after cooling. The compositions which were composed of nearly fully amorphous phase both occurred at Ln : Si : Al : O : N = 20 : (70–60) : (10–20) : 60 : 40 (Tables 4 and 5). Nevertheless, a slight difference in the liquid phase regions can still be observed. The maximum Al solubility in the Dy-liquid is slightly lower than in the Gd-liquid. The Yb-system is more similar to the Er-system, where the maximum Al solubility in the liquids further decreases. The compositions containing few crystalline phases shift towards Si- and Ln-rich side. For the Yb-system, the compositions occurred at Ln : Si : Al : O : N = (20–25) : (70–65) : 10 : 60 : 40

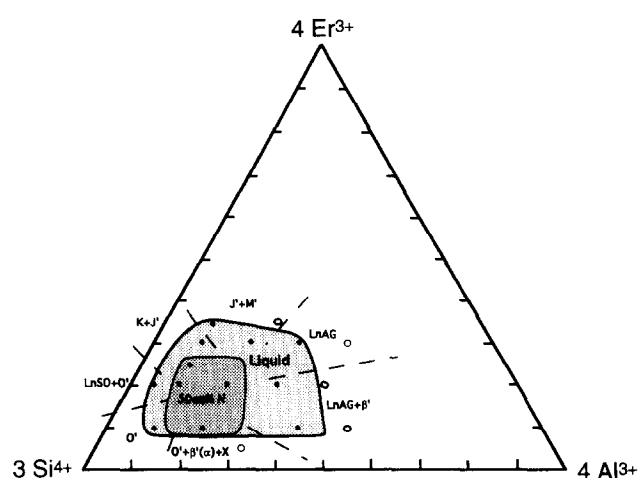


Fig. 7. Er-sialon liquid phase regions (1700°C) at 40 eq% N (with neighbouring crystalline phases indicated, LnSO :  $\beta$ - $\text{Ln}_2\text{Si}_2\text{O}_7$ , see Table 6 and Fig. 2) and 50 eq% N.

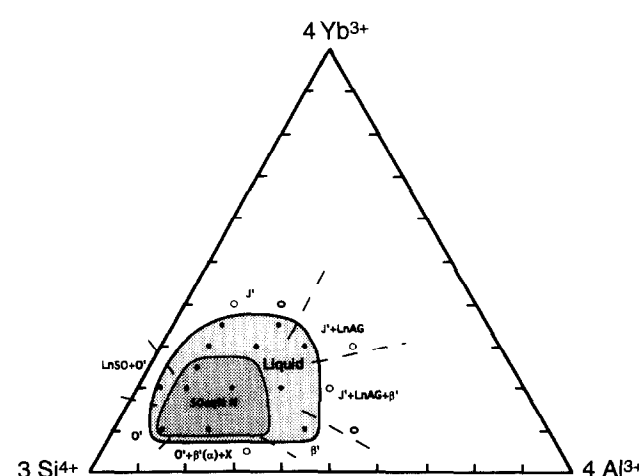


Fig. 8. Yb-sialon liquid phase regions (1700°C) at 40 eq% N (with neighbouring crystalline phases indicated, see Table 7 and preceding figures) and 50 eq% N.

(Table 7), which contains less Al than in the Ln-systems with lower Z-value rare earth elements. As mentioned before, in the Nd and Sm-systems, the amorphous phase occurred at Ln:Si:Al:O:N = 20:(60–55):(20–25):60:40. Obviously, with increasing Z-value of rare earth elements, the liquid

phase regions (at 40 eq%) contract with the glass compositions shifting slightly towards Si- and Ln-rich side. At 50 eq% N, with increasing Z-value of rare earth elements, the liquid phase regions have no obvious contraction, but shift slightly towards Si- and Ln-rich side.

**Table 4.** Compositions explored in the Gd–Si–Al–O–N system with 40 eq% N

No.	Compositions (eq%)			W.L. (wt%)	Crystalline phases*	Appearance
	Gd	Si	Al			
Gd-1	5	65	30	2.5	X w; o'w; $\beta'$ w; $\alpha$ w	half melted
Gd-2	10	80	10	2.6	o'w	melted, swollen
Gd-3	10	70	20	1.0	o'w; $\beta'$ vw; $\alpha$ vw	melted, swollen
Gd-4	10	50	40	3.9	$\beta'$ m	melted, swollen
Gd-5	10	40	50	1.0	$\beta_{60}$ m	melted, swollen
Gd-6	10	30	60	1.1	Al <sub>2</sub> O <sub>3</sub> mw; 15Rw; $\beta_{60}$ w	half-melted
Gd-7	20	75	5	1.5	o'w	melted
Gd-8	20	70	10	1.1	None (tr. $\alpha$ , $\beta'$ )	melted, swollen
Gd-9	20	60	20	1.7	None (tr. $\beta'$ )	melted, swollen
Gd-10	20	50	30	2.7	LnAlO <sub>3</sub> w; M'w; $\beta'$ vw	melted, swollen
Gd-11	20	40	40	0.4	LnAG m; M'w	melted
Gd-12	20	30	50	3.0	LnAlO <sub>3</sub> vs; $\beta'$ w	unmelted
Gd-13	25	65	10	0.1	H s	melted, swollen
Gd-14	30	60	10	0.9	H s; K m; $\beta$ w	melted, swollen
Gd-15	30	50	20	0.9	M'vs; LnAlO <sub>3</sub> m	melted
Gd-16	30	40	30	1.5	M's; LnAlO <sub>3</sub> s	melted
Gd-17	30	30	40	1.1	LnAlO <sub>3</sub> s; M'm; $\beta'$ vw	unmelted
Gd-18	35	55	10	1.1	M'vs; H w	melted
Gd-19	35	42.5	22.5	0.1	LnAlO <sub>3</sub> s; J'm	unmelted

\*J' = J-phase (YAM-type) solid solution (Ln<sub>4</sub>Si<sub>2-x</sub>Al<sub>x</sub>O<sub>7+x</sub>N<sub>2-x</sub>); LnAG = garnet-phase (Ln<sub>3</sub>Al<sub>5</sub>O<sub>12</sub>); for others see Tables 1–3.

**Table 5.** Compositions explored in the Dy–Si–Al–O–N system with 40 eq% N

No.	Compositions (eq%)			W.L. (wt%)	Crystalline phases*	Appearance
	Dy	Si	Al			
Dy-1	5	65	30	2.6	o'w; X w; $\beta'$ w; $\alpha$ vw	half-melted
Dy-2	10	80	10	3.4	o'm	melted, swollen
Dy-3	10	70	20	3.1	o'm; $\alpha$ w; $\beta$ vw	melted, swollen
Dy-4	10	50	40	3.8	$\beta'$ m	melted
Dy-5	10	40	50	2.3	$\beta'$ m; LnAG mw	half-melted
Dy-6	20	75	5	1.3	o'w	melted
Dy-7	20	70	10	2.8	None (tr. $\alpha$ , $\beta'$ )	melted, swollen
Dy-8	20	60	20	2.4	None (tr. $\beta'$ )	melted, swollen
Dy-9	20	50	30	3.6	LnAlO <sub>3</sub> m; $\beta'$ w;	melted, swollen
Dy-10	20	40	40	2.9	B m, LnAlO <sub>3</sub> m; $\beta'$ m; LnAG w	melted, swollen
Dy-11	20	30	50	2.4	LnAlO <sub>3</sub> vs; LnAG mw	unmelted
Dy-12	25	65	10	3.7	H m	melted, swollen
Dy-13	30	60	10	1.7	K s; H w	melted, swollen
Dy-14	30	50	20	0.1	M'vs; LnAlO <sub>3</sub> m	melted
Dy-15	30	40	30	0	M'vs; LnAG s; LnAlO <sub>3</sub> w	melted
Dy-16	30	30	40	2.1	J's	unmelted
Dy-17	35	55	10	1.3	M'vs; H m	melted
Dy-18	35	42.5	22.5	0.6	J'vs	melted
Dy-19	35	35	30	0.7	M'vs; LnAG m; LnAlO <sub>3</sub> w	melted
Dy-20	40	50	10	0	M's; H m	unmelted
Dy-21	40	40	20	0	M'vs; LnAG m; J'w	unmelted

\*B = B-phase (Ln<sub>2</sub>SiAlO<sub>5</sub>N); for others see preceding tables.

In order to compare with the Y–Si–Al–O–N system, the N-rich Y-sialon liquid has also been examined. No liquid was observed at 40 eq% N, then the section of 30 eq% N was further explored (see Fig. 9 and Table 8). As indicated in Fig. 9, the liquid occurred with an extension similar to the Ln-sialon liquid at 50 eq% N. The compositions Y:Si:Al:O:N = (20–30):(60–50):20:70:30 contained very little crystalline phases and are considered to be located in the glass-forming region with the highest nitrogen content. This

composition is very close to the data reported in the literature.<sup>1,11</sup> In Hampshire *et al.*'s work,<sup>1</sup> a high nitrogen glass with the composition of  $Y_{15}Si_{15}Al_{10}O_{45}N_{15}$  (Y:Si:Al:O:N = 33:44:22:66:33 in eq%) was obtained and it was suggested that one in four oxygen atoms can be replaced by nitrogen. Winder *et al.*,<sup>11</sup> by using an electron energy loss spectrometer, directly determined the intergranular glass compositions in a Y–Si–Al–O–N ceramic and reported some glass compositions, of which one with the highest N content is Y:Si:Al:

**Table 6.** Compositions explored in the Er–Si–Al–O–N system with 40 eq% N

No.	Compositions (eq%)			W.L. (wt%)	Crystalline phases*	Appearance
	Er	Si	Al			
Er-1	5	65	30	2.4	X m; o'm; $\beta'$ w $\alpha$ w	unmelted
Er-2	10	80	10	1.9	o'vs	melted, swollen
Er-3	10	70	20	3.7	o's; $\alpha$ w	melted, swollen
Er-4	10	50	40	4.0	$\beta'$ vs	melted
Er-5	10	40	50	2.1	LnAG vs; $\beta'$ m	half-melted
Er-6	20	75	5	2.1	$\beta$ -Er <sub>2</sub> Si <sub>2</sub> O <sub>7</sub> vs; o's; $\beta'$ w	melted
Er-7	20	70	10	1.7	$\alpha$ w; $\beta'$ vw	melted
Er-8	20	60	20	2.2	$\beta'$ w; $\alpha$ vw	melted
Er-9	20	50	30	2.1	LnAG vs; B m; $\beta'$ w	melted, swollen
Er-10	20	40	40	0.2	LnAG vs; $\beta'$ vw	half-melted
Er-11	25	65	10	0.7	$\alpha$ w; $\beta'$ w	melted, swollen
Er-12	30	60	10	0.8	K vs; J'mw; $\beta'$ mw	melted, swollen
Er-13	30	50	20	3.1	J'vs; $\beta'$ vw	melted
Er-14	30	40	30	2	LnAG vs; J'vw	melted
Er-15	30	30	40	0	LnAG vs; J'vw	unmelted
Er-16	35	55	10	1.2	J'vs; $\beta'$ w	melted
Er-17	35	42.5	22.5	0.9	M'vs; J'vs; LnAG m	half-melted

\*See preceding tables.

**Table 7.** Compositions explored in the Yb–Si–Al–O–N system with 40 eq% N

No.	Compositions (eq%)			W.L. (wt%)	Crystalline phases*	Appearance
	Yb	Si	Al			
Yb-1	5	65	30	3.7	$\beta'$ m; X m; $\alpha$ w	unmelted, swollen
Yb-2	10	80	10	1.6	o'vs	melted, swollen
Yb-3	10	70	20	3.8	o'vs; $\alpha$ mw; $\beta'$ w	melted
Yb-4	10	50	40	3.1	$\beta'$ s	melted
Yb-5	10	40	50	1.0	LnAG vs; $\beta_{60}$ s	half-melted, swollen
Yb-6	20	75	5	3.9	$\beta$ -Yb <sub>2</sub> Si <sub>2</sub> O <sub>7</sub> vs; o'w; $\beta'$ w	melted, swollen
Yb-7	20	70	10	0.6	$\alpha$ w; $\beta'$ vw	melted
Yb-8	20	60	20	1.4	J'vs; $\beta'$ vw	melted
Yb-9	20	50	30	3.7	LnAG m; $\beta'$ w	melted
Yb-10	20	40	40	0.5	J'vs	unmelted
Yb-11	25	65	10	3.0	$\beta'$ vw; $\alpha$ vw	melted
Yb-12	30	60	10	0.9	J'vs; $\beta'$ vw	melted
Yb-13	30	50	20	0.2	LnAG vs; $\beta'$ w	melted
Yb-14	30	40	30	4	J'vs; LnAG m	melted, swollen
Yb-15	30	30	40	1.7	J's; LnAG s	unmelted
Yb-16	35	55	10	0.7	J'vs; $\beta'$ w	melted
Yb-17	35	42.5	22.5	2.9	J'vs	melted
Yb-18	40	50	10	0.1	J'vs; $\beta'$ w; LnAG w	unmelted
Yb-19	40	40	20	0.5	J'vs; $\beta'$ vw	half-melted

\*See preceding tables.

O : N = 30 : 50 : 20 : 72 : 28. The intergranular glass compositions in Ln-sialon ceramics have not been reported in the literature, but from the agreement between the bulk glass compositions and the intergranular glass compositions directly determined in the Y-Si-Al-O-N system, the intergranular glass compositions with highest N content in the Ln-sialon ceramics can be expected. In the Nd-, Sm-sialon ceramics, the intergranular glass compositions with highest N content are expected to occur at around Nd(Sm):Si:Al:O:N = 20:60:20:60:40. For the Gd-(or Dy)-sialon and Er-(or Yb)-sialon ceramics, the compositions Gd(Dy):Si:Al:O:N = 20:(70–60):(10–20):60:40 and Er(Yb):Si:Al:O:N = (20–25):(70–65):10:60:40 are the more possible intergranular glass compositions. These compositions contain more N and less rare earth element than in the Y-Si-Al-O-N system. The crystalline phases occurring in the  $\text{Si}_3\text{N}_4$ -rich liquids, such as melilite phase(M') in the Sm-system, might also be the most possible intergranular crystalline phases in the ceramics. With increasing Z-value of rare earth elements,

LnAG( $\text{Ln}_3\text{Al}_5\text{O}_{12}$ ) becomes more stable instead of melilite solid solution(M') and  $\text{LnAlO}_3$ . In fact, M' phase easily occurs as an intergranular crystalline phase in the Ln-sialon ceramics with low Z-value Ln<sup>4,6</sup> and in the Yb-sialon ceramics  $\text{Yb}_3\text{Al}_5\text{O}_{12}$  is the stable intergranular crystalline phase.<sup>4</sup>

#### 4 Conclusions

The Ln-Si-Al-O-N (Ln = Nd, Sm, Gd, Dy, Er and Yb) systems possess extensive liquid phase regions at 40 eq% N. With increasing nitrogen, the liquid phase regions contract towards Si-rich compositions. The maximum solubility of nitrogen in the liquid phases is slightly above 50 eq% N. However, in the Y-Si-Al-O-N system, the N-rich liquid phase region is much smaller than in the Ln-Si-Al-O-N systems. The maximum solubility of nitrogen in Y-sialon liquid is slightly above 30 eq%. The liquid phase formation in the neighbouring Ln-systems is more similar. With increasing Z-value of rare earth elements, the liquid phase regions contract or shift towards Si- and Ln-rich side. The compositions Nd(Sm):Si:Al:O:N = 20:60:20:60:40, Gd(Dy):Si:Al:O:N = 20:(70–60):(10–20):60:40 and Er(Yb):Si:Al:O:N = (20–25):(70–65):10:60:40 were observed to be close to the glass-forming regions and are expected to be close to the intergranular glass compositions in the Ln-sialon ceramics.

#### Acknowledgements

This work was supported by NNSF (National Natural Science Foundation, China). The authors thank J. X. Chen and Y. X. Jia for technical assistance.

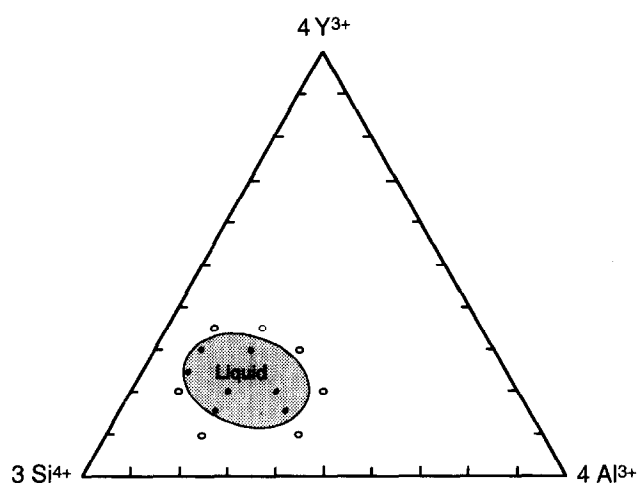


Fig. 9. Y-sialon liquid phase region (1700°C) at 30 eq% N.

Table 8. Compositions explored in the Y-Si-Al-O-N system with 30 eq% N

No.	Compositions (eq%)			W.L. (wt%)	Crystalline phases*	Appearance
	Y	Si	Al			
Y-1	10	70	20	0.4	o'vs	half-melted, swollen
Y-2	10	50	40	2.6	$\beta'$ m; mullite w	half-melted, swollen
Y-3	15	65	20	2.2	o'm	melted, swollen
Y-4	15	50	35	1.5	$\beta'$ mw	melted, swollen
Y-5	20	70	10	0.1	$\beta$ - $\text{Y}_2\text{Si}_2\text{O}_7$ vs; o's	half-melted, swollen
Y-6	20	60	20	0.5	$\beta'$ vw; $\alpha$ tr.	melted, swollen
Y-7	20	50	30	1	$\beta'$ w; $\alpha$ vw	melted, swollen
Y-8	20	40	40	1.6	YAG s; M'm; K w	half-melted, swollen
Y-9	25	65	10	2.9	$\beta$ w; $\alpha$ vw	melted, swollen
Y-10	30	60	10	0.9	$\beta'$ vw; $\alpha$ tr.	melted
Y-11	30	50	20	0.8	$\beta'$ vw	melted
Y-12	30	40	30	0	YAG vs	half-melted
Y-13	35	55	10	0.3	undetected	half-melted
T-14	35	45	20	0	undetected	unmelted

\*YAG= $\text{Y}_3\text{Al}_5\text{O}_{12}$ ; for others see preceding tables.

## References

1. Hampshire, S., Drew, R. A. L. & Jack, K.H., Oxynitride glasses. *Phys. and Chem. of Glasses*, **26**(5) (1985) 182–186.
2. Loehman, R. E., Preparation and properties of yttrium–silicon–aluminum oxynitride glasses. *J. Amer. Ceram. Soc.*, **62** (1979) 491–494.
3. Slasor, S., Liddell, K. & Thompson, D. P., The role of  $\text{Nd}_2\text{O}_3$  as an additive in the formation of  $\alpha'$  and  $\beta$ -sialon. In *Proc. Special Ceramics 8*, ed. S. P. Howlett & D. Taylor, 1986, pp. 35–50.
4. Wang, P. L., Sun, W. Y. & Yen, T. S., Sintering and formation behaviour of R- $\alpha'$ -sialons (R = Nd, Sm, Gd, Dy, Er and Yb). *Eur. J. Solid State Inorg. Chem.*, **31** (1994) 93–104.
5. Wang, H., Sun, W. Y., Zhung, H. R. & Yan, D. S. (Yen, T. S.), Preparation of R- $\alpha'$ - $\beta'$ -sialons (R = Sm, Gd, Dy, Y and Yb) by pressureless sintering. *J. Eur. Ceram. Soc.*, **13** (1994) 461–465.
6. Cheng, Y.-B. & Thompson, D. P., Preparation and grain-boundary devitrification of samarium  $\alpha$ -sialon ceramics. *J. Eur. Ceram. Soc.*, **14** (1994) 13–21.
7. Sun, W. Y., Yan, D. S., Gao, L., Mandal, H., Liddell, K. & Thompson, D. P., Subsolidus phase relationships in the systems  $\text{Ln}_2\text{O}_3$ – $\text{Si}_3\text{N}_4$ – $\text{AlN}$ – $\text{Al}_2\text{O}_3$  (Ln=Nd,Sm). *J. Eur. Ceram. Soc.*, **15** (1995) 349–355.
8. Thompson, D. P., New grain-boundary phases for nitrogen ceramics. In *Mat. Res. Soc. Symp. Proc. Symposium K*, vol. 287, ed. I.-W. Chen et al. MRS, 1993, pp. 79–92.
9. Tu, H. Y., Sun, W. Y., Wang, P. L. & Yan, D. S., Glass-forming region in the Sm–Si–Al–O–N system. *J. Mater. Sci. Lett.*, **14** (1995) 1118–1122.
10. Sun, W. Y., Yan, D. S., Gao, L., Mandal, H. & Thompson, D. P., Subsolidus phase relationships in the system  $\text{Dy}_2\text{O}_3$ – $\text{Si}_3\text{N}_4$ – $\text{AlN}$ – $\text{Al}_2\text{O}_3$ . *J. Eur. Ceram. Soc.* (in press).
11. Winder, S. M. & Lewis, M. H., Nitrogen content of the intergranular glass phase in Sialon ceramics. *J. Mater. Sci. Lett.*, **4** (1985) 241–243.